NASA TECHNICAL MEMORANDUM

NASA TM-76715

THE CALCULATION OF SEPARATED FLOW AT HELICOPTER BODIES

G. Polz

Zur Berechnung der abgelösten Strömung an Hubschrauberrümpfen, Messerschmitt-Bölkow-Blohm GmbH, Munich, W. Germany, DGLR no. 81-026, May 1981, 26 pages

NATIONAL AERONAUTICS AND SPACE ADMINISTRATION
WASHINGTON D.C. 20546
MAY 1982

STANDARD TITLE PAGE

1. Report No.	2. Government Accession No.	3. Recipient's Catalog No.
NASA TM-76715		

4. Title and Subtitle	5. Report Date
The Calculation of Separated Flow at Helicopter Bodies	May 1982
	6. Performing Organization Code

7. Author(s)	8. Performing Organization Report No.
G. Polz, MBB-Munich	10. Work Unit No.

9. Performing Organization Name and Address	11. Contract or Grant No.
Leo Kanner Assoc., Redwood City, CA 94063	NASw 3541
	13. Type of Report and Period Covered
	Translation
12. Sponsoring Agency Name and Address	14. Sponsoring Agency Code
National Aeronautics and Space Administration, Washington, DC 20546	

15. Supplementary Notes

Translation of Zur Berechnung der abgelösten Strömung an Hubschrauberümpfen, Messerschmitt-Bölkow-Blohm GmbH, Munich, W. Germany, DGLR no. 81-026, May 1981, 26 pages (A81-47555)

16. Abstract

In the case of helicopters, it is not always possible to avoid flow separation with wake formation at the rear of the fuselage. The wake region makes an analytical computation of the flow with the methods of the potential theory impossible. A survey of existing procedures for separated fuselage flows is provided, and a description is given of a computational model which is based on a combination of panel and boundary-layer computational procedures. The model makes use of a trailing body with uniform circulation distribution to simulate the wake region. The possibilities provided by the procedure are illustrated with the aid of pressure distribution and flowfield calculations. Results obtained in wind tunnel and flight tests are also shown.

17. Key Words (Selected by Author(s))	18. Distribution Statement
	Unclassified--Unlimited

19. Security Classif. (of this report)	20. Security Classif. (of this page)	21. No. of Pages	22.
Unclassified	Unclassified		

NASA TECHNICAL MEMORANDUM NASA TM-76715

THE CALCULATION OF SEPARATED FLOW AT HELICOPTER BODIES

G. Polz

Zur Berechnung der abgelösten Strömung an Hubschrauberrümpfen, Messerschmitt-Bölkow-Blohm GmbH, Munich, W. Germany, DGLR no. 81-026, May 1981, 26 pages

NATIONAL AERONAUTICS AND SPACE ADMINISTRATION

WASHINGTON, D.C. 20546

May, 1982

STANDARD TITLE PAGE

1. Report No.	2. Government Accession No.	3. Recipient's Catalog No.
NASA TM76715		

4. Title and Subtitle	5. Report Date
The Calculation of Separated Flow at Helicopter Bodies	May 1982
	6. Performing Organization Code

7. Author(s)	8. Performing Organization Report No.
G. Polz, MBB-Munich	
	10. Work Unit No.

9. Performing Organization Name and Address	11. Contract or Grant No.
Leo Kanner Assoc., Redwood City, CA 94063	NASw 3541
	13. Type of Report and Period Covered
	Translation
12. Sponsoring Agency Name and Address	14. Sponsoring Agency Code
NASA, Washington, D.C. 20546	

15. Supplementary Notes

Zur Berechnung der abgelösten Strömung an Hubschrauberrümpfen, Messerschmitt-Bölkow-Blohm GmbH, Munich, W. Germany, DGLR no. 81-026, May 1981, 26 pages

16. Abstract

In the case of helicopters, it is not always possible to avoid flow separation with wake formation at the rear of the fuselage. The wake region makes an analytical computation of the flow with the methods of the potential theory impossible. A survey of existing procedures for separated fuselage flows is provided, and a description is given of a computational model which is based on a combination of panel and boundary-layer computational procedures. The model makes use of a trailing body with uniform circulation distribution to simulate the wake region. The possibilities provided by the procedure are illustrated with the aid of pressure distribution and flowfield calculations. Results obtained in wind tunnel and flight tests are also shown.

17. Key Words (Selected by Author(s))	18. Distribution Statement
	Unclassified--Unlimited

19. Security Classif. (of this report)	20. Security Classif. (of this page)	21. No. of Pages	22.
Unclassified	Unclassified		

NASA-HQ

THE CALCULATION OF SEPARATED FLOW AT HELICOPTER BODIES

G. Polz

Messerschmidt-Bölkow-Blohm GmbH, Munich, W. Germany

1. Introduction

In the design of helicopter fuselages, designs frequently result--due to the end-use of the aircraft--which are not optimal from an aerodynamic standpoint (fig. 1). For these fuselage shapes, flow separations frequently occur (fig. 2) which are noticed primarily by the resistance, and thus indirectly by the economics, and also by a deterioration in stability properties and vibrations with similar effects. Due to the observed trend in modern helicopters toward higher flight speeds, this problem--which was of subordinate importance to earlier developments--has recently moved to the foreground. The problems connected with this provided the impetus for various investigations on flow separation from helicopter fuselages, which were partly of an experimental nature to solve real problems [1,2], and partly of a theoretical nature for basic research on physical relationships [3-12].

2. Flow Separation and Wake Formation

Among the various forms of flow separation (fig. 3), for the typically compact fuselage shapes of helicopter, wake separation occurs, whereas eddy separation occurs only at extreme angles of attack. The reason for the wake separation is a relatively precipitous decrease in cross-section in the fuselage region and the retarded flow connected with it. The continuation of the boundary layer forms the wake region which contains a backflow region near the wall.

Since the flow material coming from the boundary layer is rotational or frictional, the wake contains no potential flow, which impedes a computational treatment of such flows. The rotation

present there corresponds in its effect, to a vortex distribution whose induction affects the entire flow field around the fuselage. Thus the description of wake influences is of prime importance in the determination of this induction effect.

The origination of wake circulation can be illustrated on the example of a rotation-symmetric body with incident flow (fig. 4): The entire wall boundary-layer represents a shear-flow region--since the velocity jump from u = 0 at the surface to the outside speed u = U must be overcome in it--for which the Euler equation for rotational flows can be used:

$$\vec{\omega} = \begin{vmatrix} \omega_x \\ \omega_y \\ \omega_z \end{vmatrix} = \frac{1}{2} \begin{vmatrix} \frac{\partial w}{\partial y} - \frac{\partial v}{\partial z} \\ \frac{\partial u}{\partial z} - \frac{\partial w}{\partial x} \\ \frac{\partial v}{\partial x} - \frac{\partial u}{\partial y} \end{vmatrix} \tag{1}$$

In a local coordinate system, the lateral component v and all derivatives of y disappear due to rotational symmetry; in addition $\partial w/\partial x$ can be neglected. Thus it follows that the rotation

$$\vec{\omega} = \frac{1}{2} \, (0, \; \partial u/\partial z, \; 0) \tag{2}$$

depends only on the velocity gradient. The circulation

$$\gamma_y = \frac{\partial \Gamma_y}{\partial s} = 2 \int_0^{\delta} \omega_y \cdot dz = \int_0^{\delta} \frac{\partial u}{\partial z} \, dz = \int_0^{\delta} du = U \tag{3}$$

present in the boundary layer per length unit depends only on the outside velocity U, but not on the velocity profile or on the thickness of the boundary layer. Since the circulation in a boundary layer element of length ds

$$d\Gamma_y = \oint V \cdot dl = d\phi = U \cdot ds \tag{4}$$

is equal to the change in potential $d\phi$, this means that each vortex element is bounded by two equipotential lines. From the arrangement of potential lines we can see that the entire circulation present in the boundary layer can be described by a system of closed eddy lines oriented in the circumferential direction.

The vortex intensity streaming into the wake with the boundary-layer material at the separation line

$$\frac{\partial \Gamma_A}{\partial t} = \int_0^\delta \frac{\partial u}{\partial z} \cdot u \cdot dz = \int_0^\delta u \cdot du = \frac{U_A^2}{2} \qquad (5)$$

represents the sole source for the "circumferential" circulation present in the wake. The backflow present in this region likewise leads to the formation of a boundary layer whose rotation is opposite that of the main boundary layer.

In general however, non-rotation-symmetric incident-flow states are present, connected with a cross-force (e.g. lift) acting on the body. This cross-force causes the appearance of natural vortexes whose free ends are parallel to the incident flow direction. In contrast to the typical vortex separation, these vortex filaments are present in the compact helicopter fuselage as uniformly distributed "longitudinal" circulation within the wake (fig. 2). The wake contains both a circulation oriented in the circumferential and in the longitudinal direction (fig. 5). For the generation of longitudinal circulation, the direction of flow lines at the fuselage surface directly in front of the separation line is probably decisive.

3. Previous Methods for Computing the Separated Flow from Helicopter Fuselages

Up until a few years ago, no computing methods were known for the calculation of the separated flow from general fuselage-shapes like helicopters. But recently, the development of methods was taken in hand specifically for helicopter fuselages, including efforts in the USA [3,4,5].

3.1 Simulation of the Wake by Flow from the Fuselage

An initial test was performed by Woodward [3] of the fuselage surface lying in the wake region by using an additional source distribution (for the fuselage itself the panel method [14] based on a source distribution of the surface was already used). A

similar method was developed by Jacob [13] for computing the separated flow from profiles. This method does permit a sufficiently accurate determination of the pressure distribution on the fuselage surface, but the pulse depression and thus the flow conditions in the far wake thus cannot be reproduced with it. A satisfactory agreement with measured results could only be achieved (fig.6) when only a part of the fuselage surface lying in the separation region was occupied by additional sources. The source strength was determined for each of the affected panels by the equation:

$$\vec{v}_s \cdot \vec{n} = \vec{v}_\infty \cdot \vec{n} \qquad (6)$$

i.e. the normal component of the velocity induced by the source was set equal to the normal component of the incident-flow velocity.

3.2 Wake Simulation with Vortex Distribution

Another method which permits a more realistic simulation of the wake was developed by Dvorak et al. [4,5]. The fuselage is again represented by panels and a vortex surface lying parallel to the incident-flow direction is first set at the panel edge lying closest to the separation line (fig. 7). The circulation of this vortex surface is determined by a control point on that surface. The length L of the vortex element is selected so that the velocity along the vortex surface remains constant in a certain range, which requires an iterative computation of the final pressure distribution. Characteristic of the results is an excessively stressed pressure increase in the region in front of the point of separation. Otherwise, a relatively accurate reproduction of the measured pressure distribution is possible.

4. Development of a Computational Model with Uniform Vortex Distribution in the Wake

Within the frame of a ZTL-contract, the development of an in-house computational method was begun at MBB for separated flows from helicopter fuselages, with the emphasis being placed on the simulation of flow states in the far wake.

4.1 Theoretical Model

The singularity methods used in flow mechanics are all based on an integral formula of the form:

$$\frac{\vec{n}}{4\cdot\pi\cdot U_\infty} \cdot \nabla \iint_{(s)} \sigma(s) \cdot \frac{ds}{r(s,p)} = \vec{n} \cdot \frac{\vec{U}_\infty}{U_\infty}, \qquad (7)$$

Singularity — Influence function — Boundary condition

which cannot be solved for the general case. It can be solved only be breaking it down into individual elements, e.g. of the surface of the body. Since just as many boundary conditions as singularities are present, a closed solution to the integral equation is possible via a linear equation system. In the case of a separated flow, the left side of the equation is expanded by the influence of the circulation contained in the wake ω (fig. 8). This circulation cannot be determined by additional equations--in contrast to the case for an airplane wing--since neither its geometry nor its boundary conditions are known. But its calculation is possible by an iterative solution to the equation system by including in the boundary calculation, the induction of the wake circulation at each control point. Since this induction effect is not known from the beginning, it must be assumed in a suitable manner, for the first iteration step. Then with the first solution for the singularity distribution, the geometry and circulation distribution of the wake can be determined--with additional appropriate assumptions.

4.2 Structure of the Computational Method

In accord with the presumptions of the theoretical model, the computational method consists of several program segments (fig. 9): The compression effect of the fuselage is computed with a panel method [14,15] which is based on a source distribution of the fuselage surface. By interpolation of the velocity distribution obtained with it, a number of flow lines is determined on the fuselage surface. For each of these flow lines, the separation

point and the boundary-layer thickness present there are determined by a 2D-boundary-layer method [16]; in this case, the fuselage is replaced for each flow line by an equivalent rotation body. The line connecting the individual separation points represents the front edge of a trailing body which is set on the fuselage and covered by a defined circulation. The frame of this trailing body is formed by the free flow lines whose starting points are away from the fuselage surface by the thickness of the boundary layer and lie above the separation points of the flow lines. Since flow material is continually moved from the outside flow into the wake due to friction effects, the wake's cross-section continually increases compared to these flow lines. The circulation present in the trailing body again affects the singularity distribution of the fuselage. Since the influence of the wake is not known in advance, the calculation of the flow state requires an iteration process which uses a prismatic trailing body of constant cross-section for the first step.

4.3 Geometry and Circulation Distribution of the Trailing Body

Wake Geometry

For the determination of the spread of the wake, the Prandtl mixing-path theorem can be used. The application of this theorem to the wake of different, blunt bodies [17] shows that the formulas based on it for the cross-sectional increase in a rotation-symmetric wake (fig. 10):

$$\frac{r}{r_A} \sim \left[\frac{x - x_o}{r_A}\right]^{1/3} \tag{8}$$

and the pertinent pulse indentation depth:

$$\frac{\Delta U}{U_\infty} \sim \left[\frac{x - x_o}{r_A}\right]^{-2/3} \tag{9}$$

are valid for bodies of finite thickness only from a certain distance x_o from the separation line, i.e. when the disturbance has already decayed due to the compression action of the body.

There is no information available about the region near the body. Since the frictional wake-flow is continually enhanced by flow material from the outside flow only from the separation line, the wake cross-section must increase compared to the flow lines forming at the separation line toward the outside edge of the wake. For a numeric determination of cross-sectional development, the equation

$$\frac{r}{r_o} = (1 + m)^{\frac{x - x_o}{r_A}} \qquad (10)$$

is selected; with m = 0.03 ... 0.05, it gives useable trailing-body shapes.

Circumferential and Longitudinal Vortex Circulation at the Separation Line

It seems useful to use, in accord with section 2, the velocity components present in the meridian-section to determine the circumferential vortex, and the circumferential components to determine the longitudinal vortex. But unfortunately, the used boundary-layer computation method (applies precisely only for rotation bodies) does not always give the precise flow direction at the separation line, which is why a sufficiently accurate determination of longitudinal circulation is not possible in this case. On the other hand, when the zero-lift direction of the fuselage is known, the middleline of the trailing body which is sloped to the incident flow direction by ca. $\alpha_i = (\alpha - \alpha_o)/2$, can be determined. From the angle between the incident-flow direction and wake midline, a circumferential component U_u can be determined (fig. 11) which leads to realistic values for the circumferential circulation.

Circulation Distribution in the Trailing Body

A sufficiently accurate determination of the wake circulation is impossible due to the numerous unknowns (local flow direction, location and intensity of the individual vortices); thus one must rely mostly on empirical assumptions. At the separation line, the circumferential circulation is given by the difference between U = 0 at the fuselage surface and the velocity U_A prevailing at the edge of the boundary layer (fig. 12, position A). Under the assumptions of eq. (2), there results a parabolic circulation distribution $\omega(z)$. Upstream from this (position B), a larger velocity difference is present due to the backflow, but this is again partly decreased by the wall boundary-layer of the backflow. For the circulation distribution this means that besides an intensive circulation in the outer layer of the wake, a weaker, opposite-rotating circulation is present near the wall. Behind the body there is generally a backflow region (C), which is why the velocity jump and thus the total circulation must be greater than at the separation line, assuming a nearly constant outside velocity U along the wake-mantle line. Outside the backflow region, the velocity difference and thus the circulation decreases gradually in accord with the Prandtl exchange law (D). A quantitative determination of the circumferential circulation along the wake axis is impossible due to these considerations.

Assuming that a similar velocity profile is present in the entire wake (with the exception of the fuselage region) as at the separation line--which is at least qualitatively correct--the same parabolic circulation distribution can be postulated everywhere.

No quantitative statements are possible about the distribution of longitudinal circulation along the wake axis. But it can be asumed that it decreases gradually from the separation line due to frictional effects. For the radial distribution of longitudinal circulation, the same parabolic profile can be assumed as for the circumferential circulation. Otherwise, with respect to the circulation distribution of the trailing body, one must still rely on experiments.

Calculation of the Static Pressure

The flow in the wake has a lower energy level than the outside flow, which is why the Bernoulli equation cannot be used here to compute the static pressure. This energy difference is computed from the velocity difference or from the circulation intensity γ of the eddy-layer which separates the considered field point from the outside flow; thus, the static pressure in the wake results as:

$$c_p = 1 - \left(\frac{V}{U_\infty} + \frac{\gamma}{U_\infty}\right)^2 \qquad (11)$$

Numeric Calculation of the Wake Induction

For this calculation, the spatially distributed circulation distribution of the irregularly shaped trailing body is replaced by suitable vortex elements. The geometric division of the trailing body defined by its mantle lines takes place through cut planes perpendicular to its longitudinal axis whose position in the body region is specified by the separation points of the individual flow lines, whereas behind the body, an equidistant cut-distribution is selected. Each cut surface represents a polygon which is subdivided into individual triangles by radial rays to the vertex points (fig. 13). The ring-like circumferential vortex distribution of the cut surfaces is replaced, for each triangle, depending on its distance to the particular field point, by one or more line vortices lying parallel to the outside edge of the triangle. The longitudinal vortex distribution of each triangular tube composing the trailing body, is viewed as constant. It too, is represented by one or more line vortices. To avoid singularity problems at field points lying close to or in the trailing body, additional cut planes are placed near the particular field point at a precisely defined distance to the field point. For the same reason, the distribution of vortex elements in each triangle is specified in accord with the position to the field point.

4.4 Results and Comparison with Measurements

Figures 14 and 15 show the pressure distribution and the flow

field of a sphere at Re = $0.45 \cdot 10^6$. With a circulation intensity constant at up to about one sphere-radius behind the separation line and then decreasing linearly, the best agreement was achieved here with the measured results. The pressure increase occurring in the calculation in the region of the separation point is attributable to the fact that the front edge of the trailing body acts like a step on the outside flow. An even better agreement with the measurements is obtained when the static pressure prevailing at the outside edge of the trailing body is used also for the sphere surface. The flow field (fig. 15) shows an at least qualitatively meaningful wake geometry with a backflow region.

Figure 16 shows the location of the separation line at the BO 105 fuselage at different angles of attack by measuring and calculation with and without wake influence. Although no longitudinal circulation was taken into account here, the results (obtained after two iteration steps) generally agree with the measurements, at least for negative angles of attack.

In figure 17 the fuselage flow lines and the trailing body including the pulse indentation are presented for the fuselage of the BK 117 at $\alpha = -5°$. The deflection of the fuselage flow lines discernable in front of the separation line does not correspond to the profile obtained in the wind tunnel test (fig. 22), but the separation line is reproduced almost correctly. The trailing body consists of 15 flow lines; this figure has also proven useful in other calculations. There are no measurements of the velocity distribution in the wake, but the resistance computed from it corresponds rather accurately to the value measured in the wind tunnel. In the computation of the pressure distribution, there is a better agreement with measurements (fig. 18) than for the pure computation based on potential theory. The fluctuations in the pressure profile discernable in the BCL behind the separation line are caused by the local circulation distribution.

Most recently, the method was used within the frame of an

investigation on optimum design of transport helicopter airframes [11] where the relatively detailed wake measurements were performed. Figure 19 shows the panel distribution for the wind tunnel model used in the calculation. In fig. 20, the profile of fuselage flow lines and the separation line from calculation and measurement are compared. Whereas the separation line is reproduced very well, the flow lines of the calculation are not sloped downward enough in the region of the separation line. With the longitudinal circulation defined in sec. 4.3, there results a velocity field in the wake cross-section lying directly behind the tail boom attachment, which comes very close to the measured one (fig. 21).

4.5 Further Development of the Method

Due to the unknown flow processes in the wake which are also almost always instationary, when applying the method an empirical adaptation of the individual parameters like wake spreading and circulation distribution, is needed. This is due primarily to the absence of suitable test results which would permit an adaptation of the computational model. But it is expected that the investigations of helicopter fuselages [11] begun last year in the DFVLR will permit a much better insight into the flow conditions prevailing in the wake. The results achieved to date represent considerable progress.

In order to give an insight into the actual problems of flow separation in helicopters, two results from wind tunnel and flight tests are provided: Figure 22 shows results from painting tests on the BK 117-model, both with and without spoiler on the fuselage rear. Due to the spoiler, the downward pressure present in the fast-flight state is reduced and the vortex pair connected with the downward pressure is moved downward which improved the flow conditions in the area of the tail unit. (In the meantime, the spoiler on the BK 117 has been replaced by another solution). The computational description of the spoiler is connected with considerable problems, in part because of the complicated panelling.

Figure 23 comes from the flight testing of the BK 117 and clearly shows the various zones of separated flow by means of the wool threads. Besides the rear of fuselage where the separation is still intensified by the spoiler, above all the fuselage top behind the rotor shaft and parts of the tail surface are affected. The picture clearly shows that some development effort is still needed for a complete theoretical description of the separated flow at the helicopter airframe.

5. Summary

The function-induced shapes and additionally occurring unfavorable incident-flow states are the principle causes for flow separations from helicopter fuselages. Due to these separation processes, both the resistance is increased and the effectiveness of controls in the tail section is reduced.

The processes of flow separation are explained, specifically with respect to the compact-shaped helicopter fuselage shapes, with emphasis on the circulation contained in the wake. In addition, the existing methods where the wake simulation uses relatively simple means, are presented. Finally, a computational model is presented which operates with a uniform circulation distribution of the wake. The equation on which the method is based, the program run and the calculation of the influence of the wake are explained. The results include both pressure distributions and flow-line profiles and flow patterns and partly show a good agreement with measurements. On the basis of practical examples, the necessity of further development of such methods is demonstrated.

REFERENCES

1. P.F. Sheridan, R.P. Smith: Interactional Aerodynamics--A new Challenge to Helicopter Technology. 35th Annual National Forum of the American Helicopter Society, Preprint No. 79-59.

2. P. Roesch: Aerodynamic Design of the Aerospatiale SA 365 N-Dauphine 2 Helicopter. 6th European Rotorcraft and Powered Lift Aircraft Forum, Bristol 1980, Paper No. 28.

3. F.A. Woodward, F.A. Dvorak, E.N. Geller: A Computer Program for Three-Dimensional Lifting Bodies in Subsonic Inviscid Flow. USAAMRDL-TR-74-18.

4. F.A. Dvorak, B. Maskew, F.A. Woodward: Investigation of Three-Dimensional Flow Separation of Fuselage Configurations. Final Report for Period May 1975 - May 1976. USAAMRDL-TR-77-4.

5. D.R. Clark, F.A. Dvorak, B. Maskew, J.M. Summa, F.A. Woodward: Helicopter Flow Field Analysis. Final Report for Period April 1977 - Sept. 1978, USARTL-RT-79-4.

6. D.R. Clark: A Study of the Effect of Aft Fuselage Shape on Helicopter Drag. 6th European Rotorcraft and Powered Lift Aircraft Forum, Bristol 1980. Paper No. 50.

7. R. Stricker, W. Gradl, G. Polz: Aerodynamic Working Principles for Future Helicopter Developments (Rotor Streaming, Separated Flow at the Fuselage, Rotor-Wing Interference). MBB GmbH, Report no. UD-194-76, 1977.

8. R. Stricker, G. Polz: Aerodynamic Working Principles for Future Helicopter Developments (Fuselage Aerodynamics, Rotor blade Optimization, Rotor-Airframe Interference). MBB GmbH, Report no. UD-228-77, 1978.

9. R. Stricker, G. Polz, W. Gradl, D. Hummes, B. Junker: Aerodynamic Working Principles for Future Helicopter Developments (Rotor-Fuselage Interference, Rotor Streaming). MBB GnbH, Report no. UD-262-78, 1979.

10. G. Polz, W. Gradl: Aerodynamic Working Principles for Future Helicopter Developments (Rotor-Fuselage Interference, Rotor Streaming) MBB GmbH, Report no. UD-289-79, 1980.

11. G. Polz, J. Quentin, A. Kühn: Wind Tunnel Investigations on the Optimum Structure of Transport Helicopter Airframes with Regard to Power Consumption and Stability Behavior. MBB Report UD-290-80, 1981.

12. R. Stricker, G. Polz: Calculation of the Viscous Flow Around Helicopter Bodies. 3rd European Rotorcraft and Powered Lift Aircraft Forum, Aix-en-Provence 1977, Paper no. 43.

13. K. Jacob: Program to Calculate the Pressure Distribution for any Profiles in Incompressible Flow with Separation or Cavitation. AVA Report 68 R 4 (1968).

14. W. Kraus, P. Sacher: The MBB Subsonic Panel Method. MBB GmbH, Report nos. UFE 632-70, UFE-633-70 and UFE 634-70 (1970).

15. W. Kraus: Further Development of the panel Method. MBB GmbH, Report no. UFE 1017 (ö) 1973.

16. J.C. Rotta: FORTRAN IV Computer program for Boundary Layers in Compressable, Smooth and Axis-symmetric Flows. DFVLR Research report 71-51.

17. H. Reichardt, R. Ermshaus: Pulse and Heat Transfer in Turbulent Wind Shadows behind Rotating Bodies. Int. J. Heat Mass Transfer, Vol. 5, 1962, pp. 251-265.

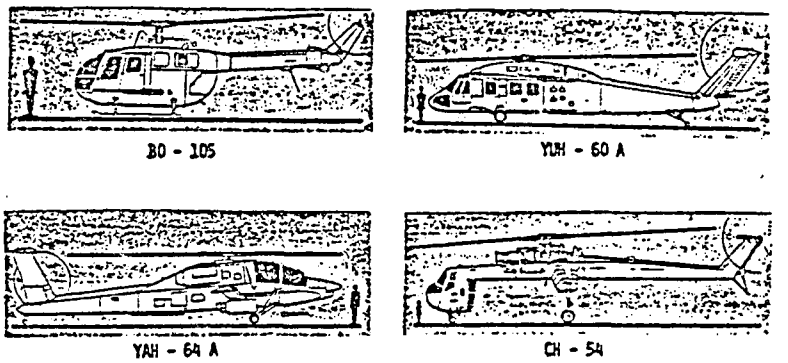

Figure 1: Typical Fuselage Shapes of Helicopters

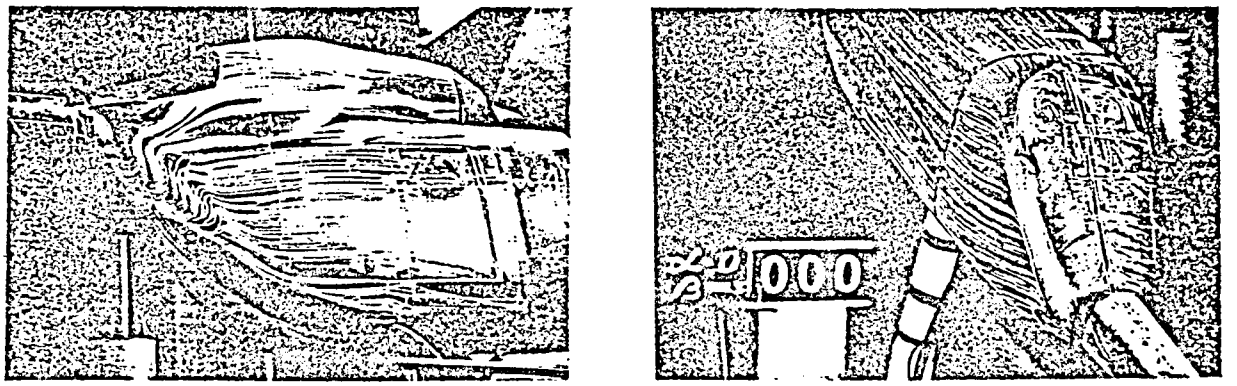

Figure 2: Separation Phenomena at Helicopter Fuselages

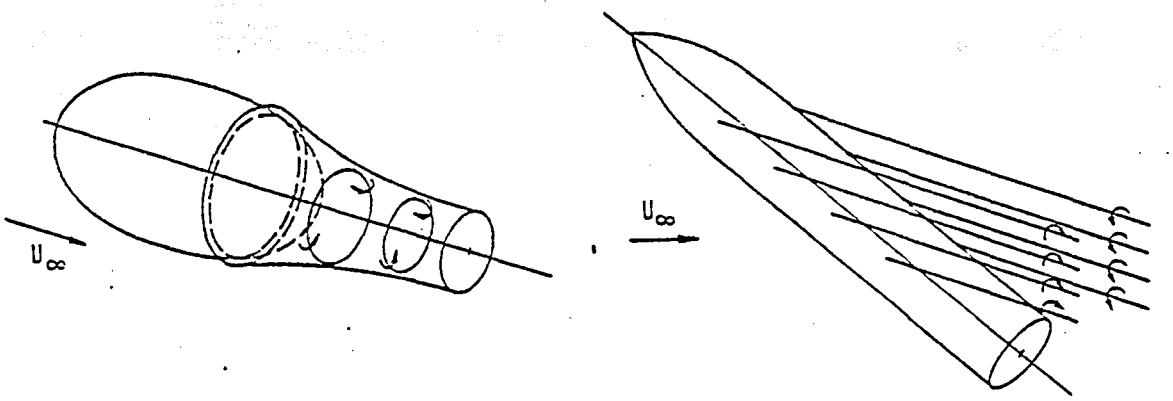

Wake separation Vortex-layer Separation

Figure 3: Wake and Vortex-Layer Separation

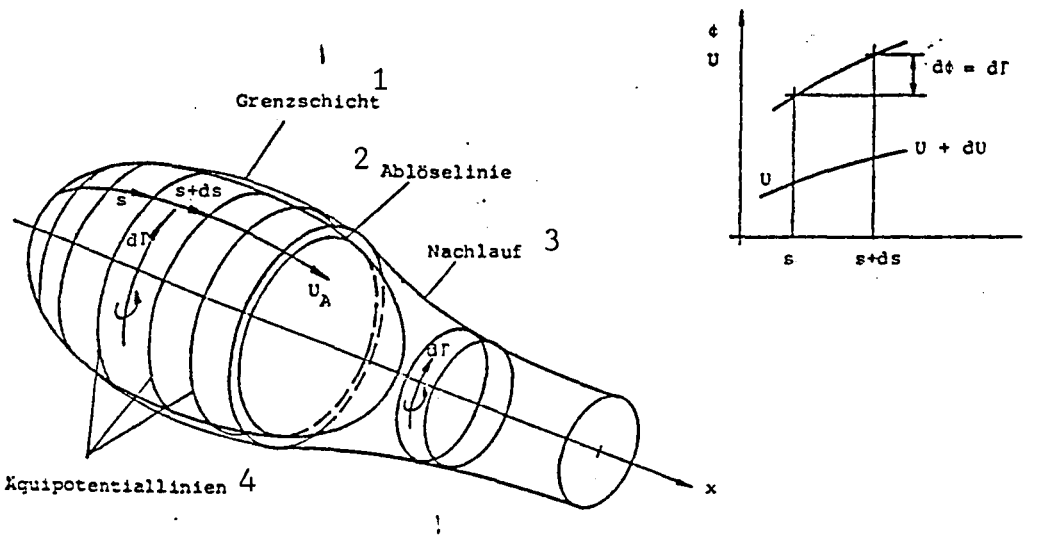

Figure 4: Generation of Wake Circulation

Key: 1-boundary layer 2-separation line 3-wake 4-equipotential lines

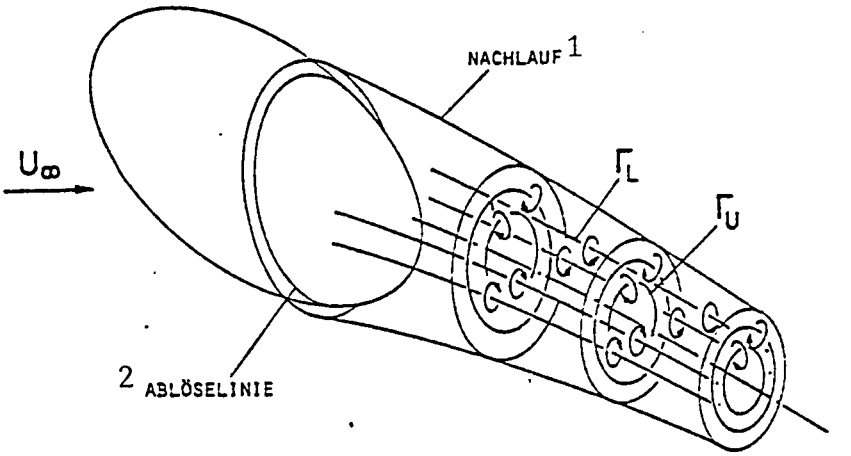

Figure 5: Vortex Distribution of the Wake

Key: 1-wake 2-separation line

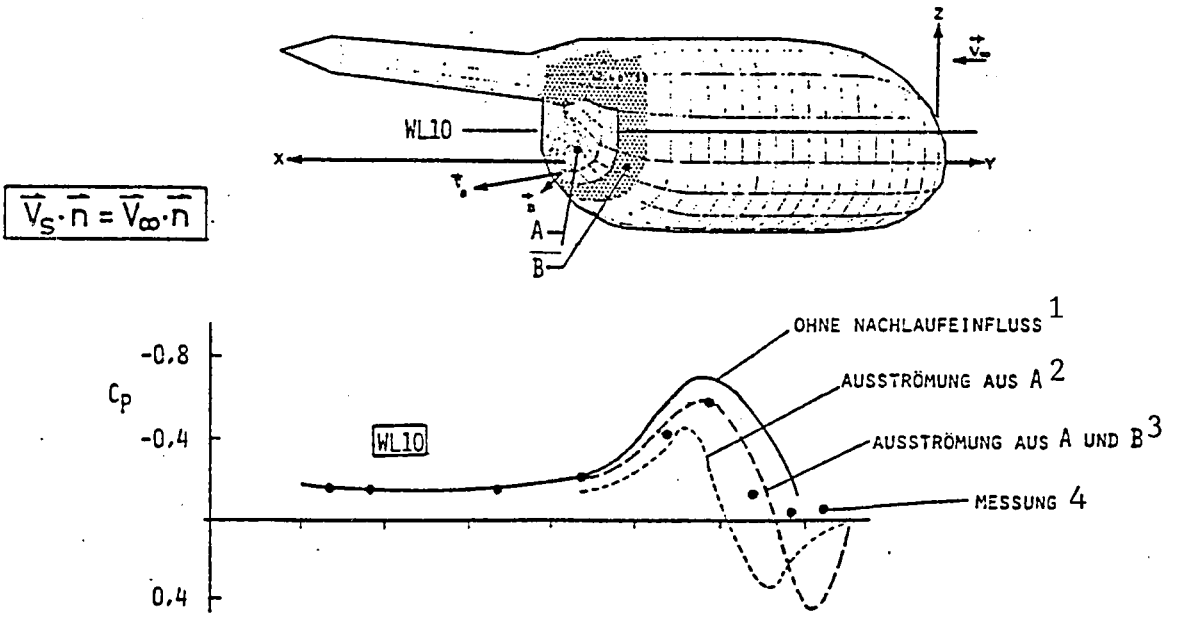

Fig. 6: Simulation of the Wake by Flow From the Fuselage Body

Key: 1-without influence of wake 2-flow from A 3-flow from A and B
4-measurement

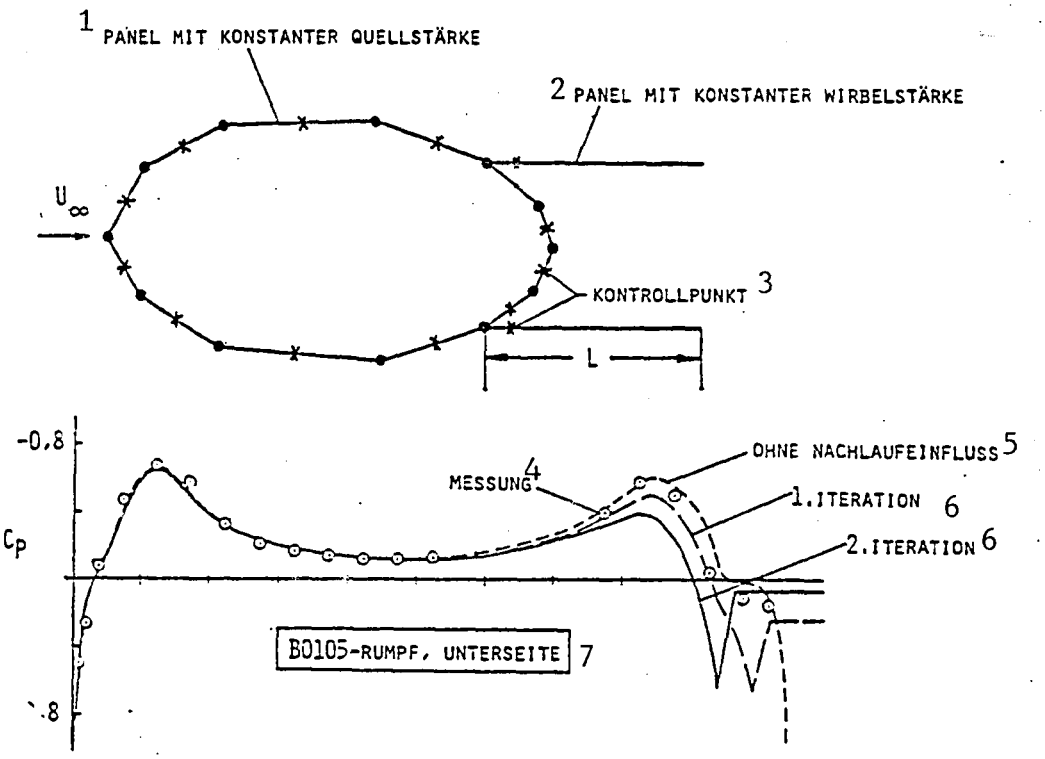

Fig. 7: Computational Model with Vortex Distribution of the Wake Outside Edge

Key: 1-panel with constant source strength 2-panel with constant vortex strength 3-control point 4-measurement 5-without the influence of wake 6-iteration 7-fuselage, underside

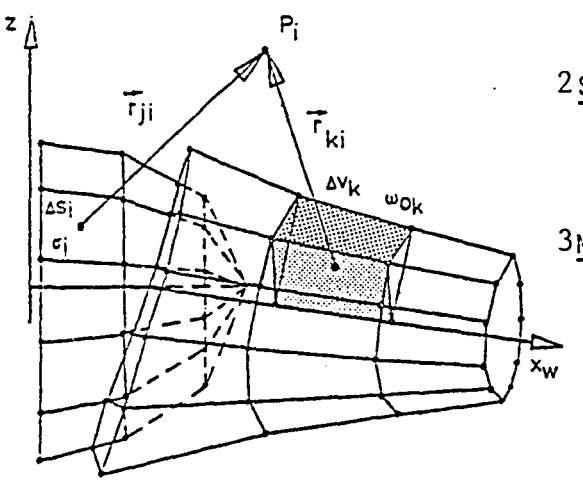

1 INTEGRALGLEICHUNG

$$\frac{\vec{n}}{4\pi u_\infty}\cdot\left[\nabla\iint_{(s)}\frac{\sigma(s)}{r(s,p)}\,ds+\iint_{(v)}\omega(v)\frac{\vec{e}_\omega\times\vec{r}(v,p)}{r(v,p)^3}\,dv\right]=\vec{n}\cdot\frac{\vec{u}_\infty}{u_\infty}$$

2 SUMMENGLEICHUNG

$$\frac{\vec{n}}{4\pi u_\infty}\nabla\sum_{(s)}\sum\frac{\sigma}{r}\cdot\Delta s=\vec{n}\left[\frac{\vec{u}_\infty}{u_\infty}-\frac{1}{4\pi u_\infty}\sum_{(v)}\sum\sum\frac{\omega_0}{r^3}\cdot\Delta v\right]$$

3 NICHTLINEARES GLEICHUNGSSYSTEM

$$[A_{ij}]\{x_j\}=\{B_i\}$$

$$A_{ij}=\vec{n}_i\cdot C_{ij}$$

$$x_j=\frac{\sigma_j}{4\pi u_\infty}$$

$$B_i=-\vec{n}_i\cdot\frac{\vec{u}_\infty}{u_\infty}+\vec{n}\sum_k\omega_{0_K}\cdot\vec{D}ik$$

Fig. 8: Numeric Solution to the Integral Equation for the Wake Flow

Key: 1-integral equation 2-sum equation 3-non-linear equation system

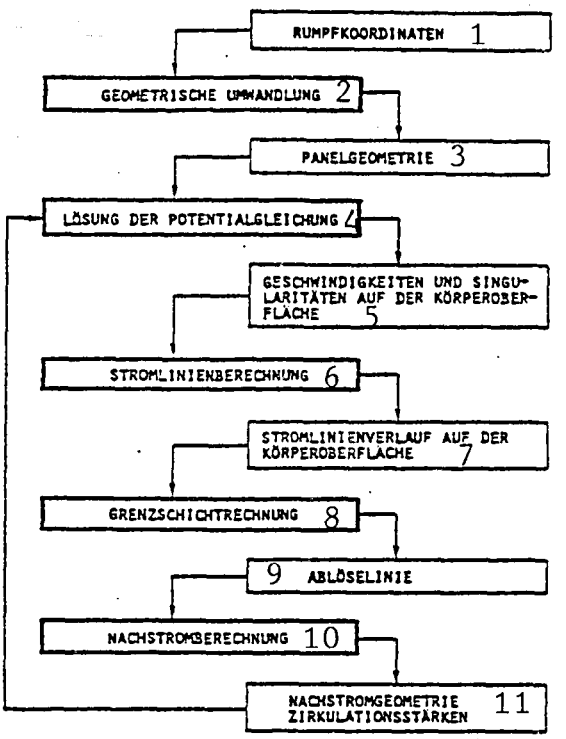

Figure 9: Program Outline of the Computation Method for Separated Flow

Key: 1-fuselage coordinates 2-geometric conversion 3-panel geometry 4-solution of the potential equation 5-velocities and singularities on the body's surface 6-flow line computation 7-flow line profile on the body's surface 8-boundary layer calculation 9-separation line 10-after-flow calculation 11-after-flow geometry, circulation intensities

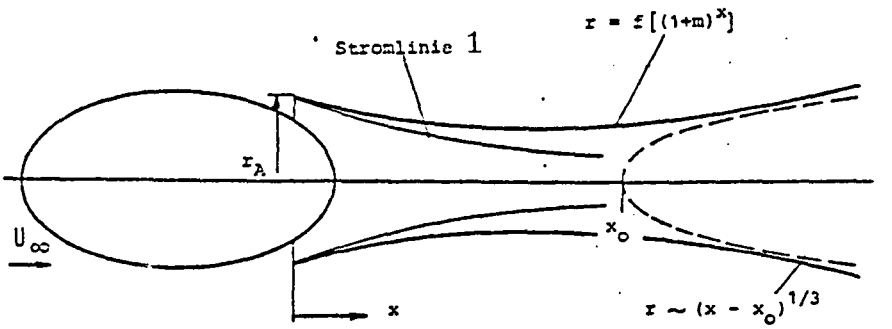

Figure 10: Geometry of the Trailing Body

Key: 1-flow line

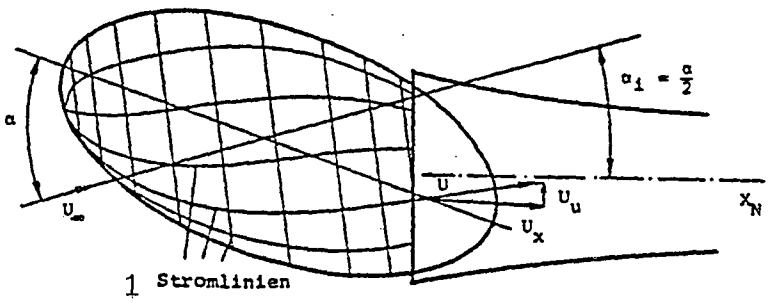

Fig. 11: Determination of the Circumferential and Longitudinal Vortex Circulation

Key: 1-flow lines

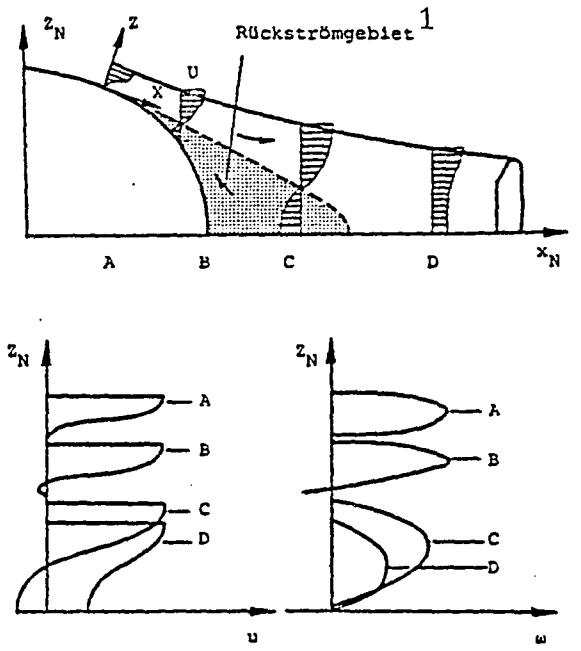

Fig. 12: Velocity and Circulation Distribution in the Wake

Key: 1-backflow region

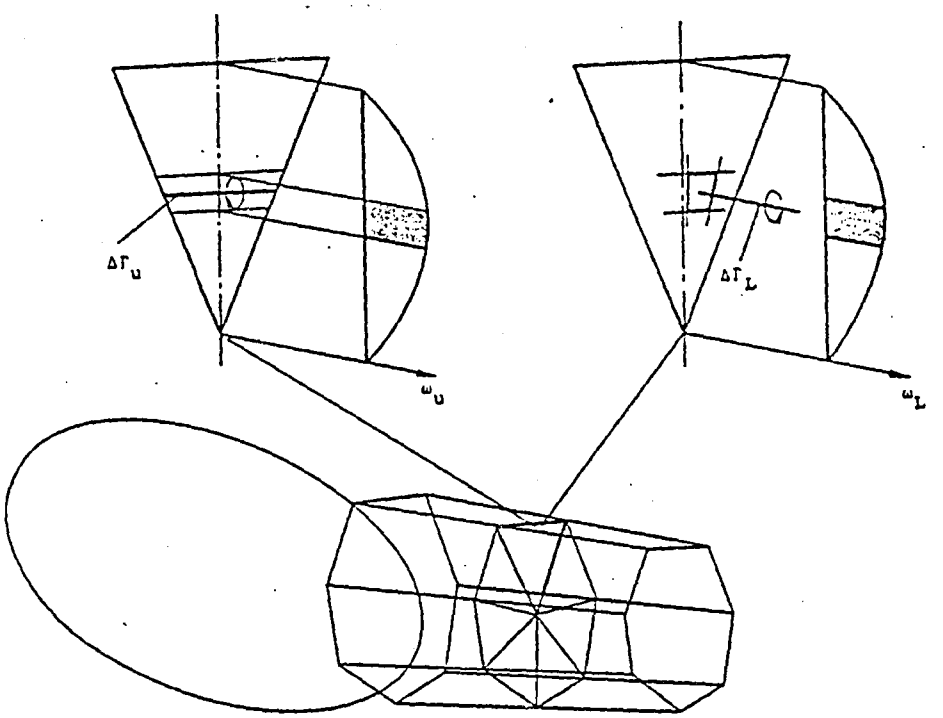

Figure 13: Calculation of Vortex Induction

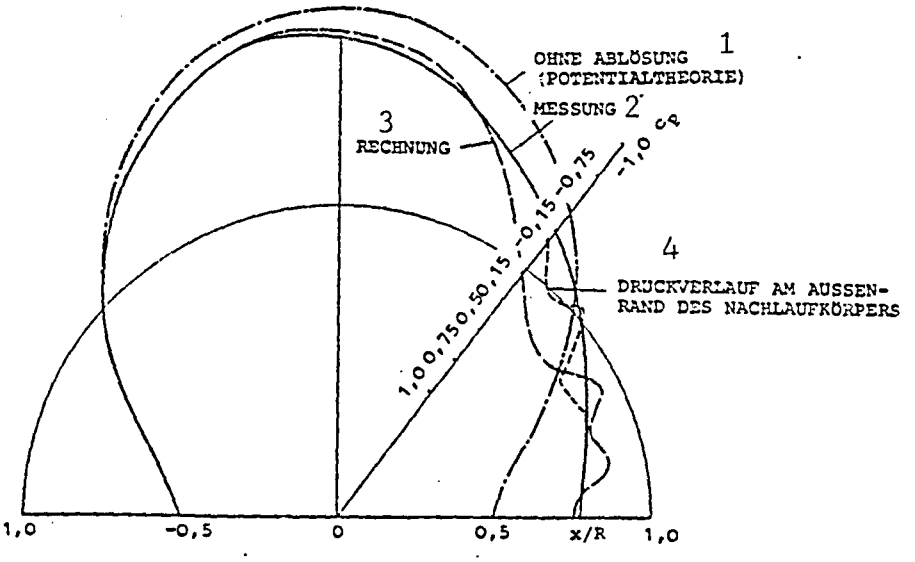

Fig. 14: Pressure Distribution on the Sphere after Calculation and Measurement ($Re = 0.45 \cdot 10^6$)

Key: 1-without separation (potential theory) 2-measurement 3-calculation 4-pressure profile at the outside edge of the trailing body

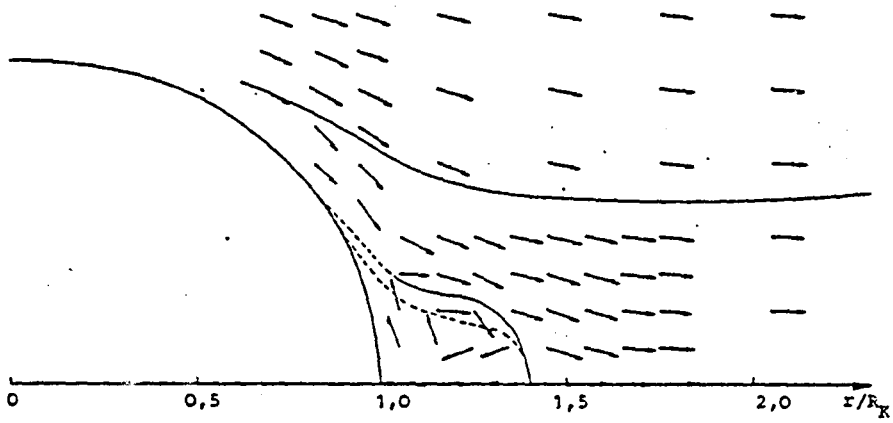

Figure 15: Velocity Field of the Separated Flow on the Sphere
(Re = $0.45 \cdot 10^6$)

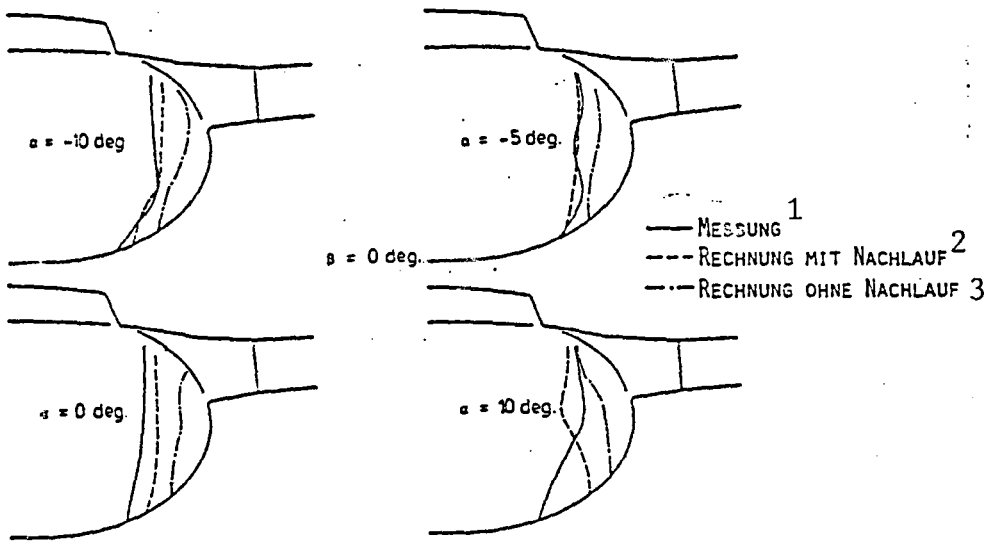

Figure 16: Separation Lines at the BO 105 Fuselage
Key: 1-measurement 2-calculation with wake 3-calculation without wake

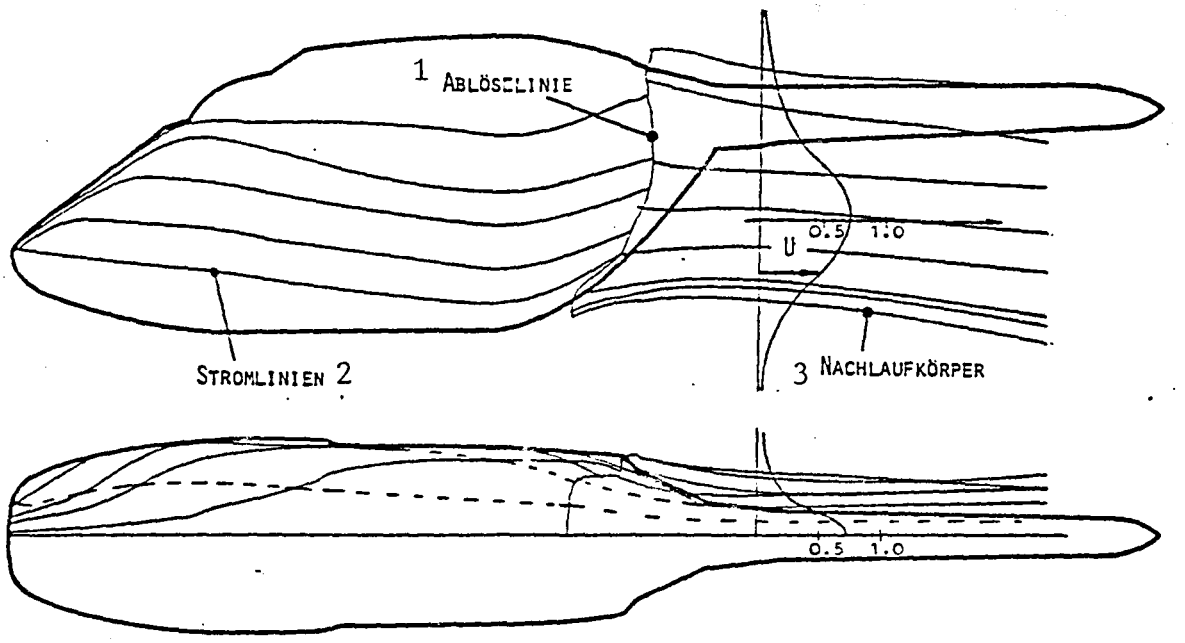

Fig. 17: BK 117 - Fuselage with Trailing Body

Key: 1-separation line 2-flow lines 3-trailing body

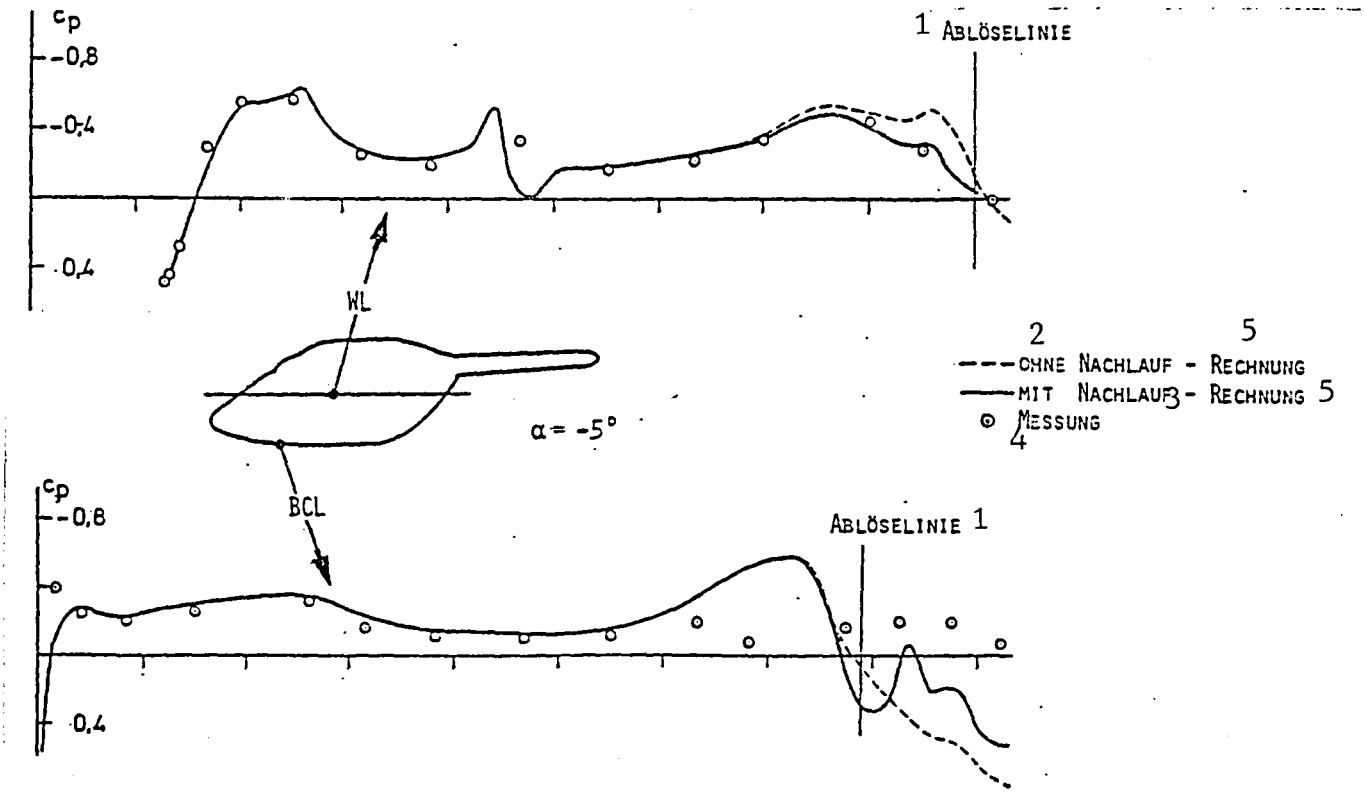

Fig. 18: Pressure Distribution on the BK 117 - Wind Tunnel Model

Key: 1-separation line 2-without wake 3-with wake 4-measurement 5-calculation

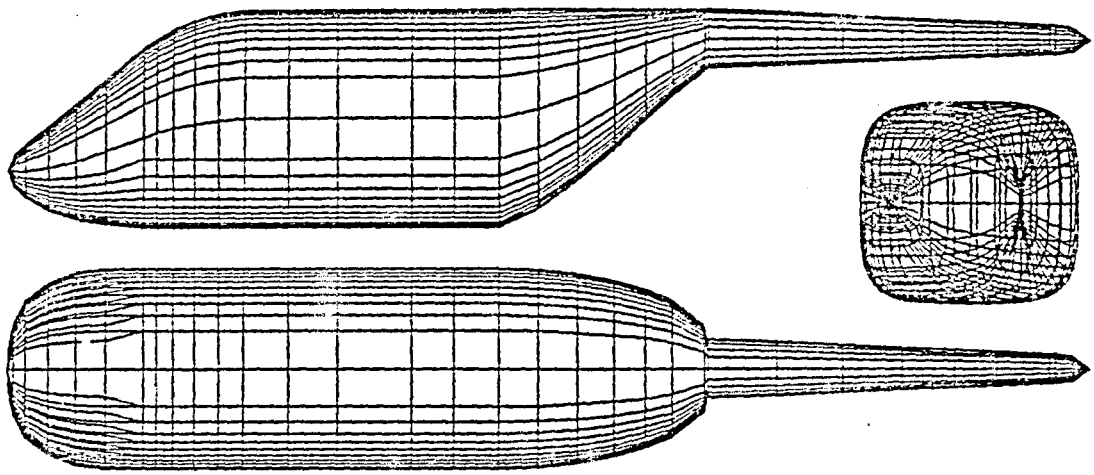

Fig. 19: Panelling of the Transport Helicopter Model

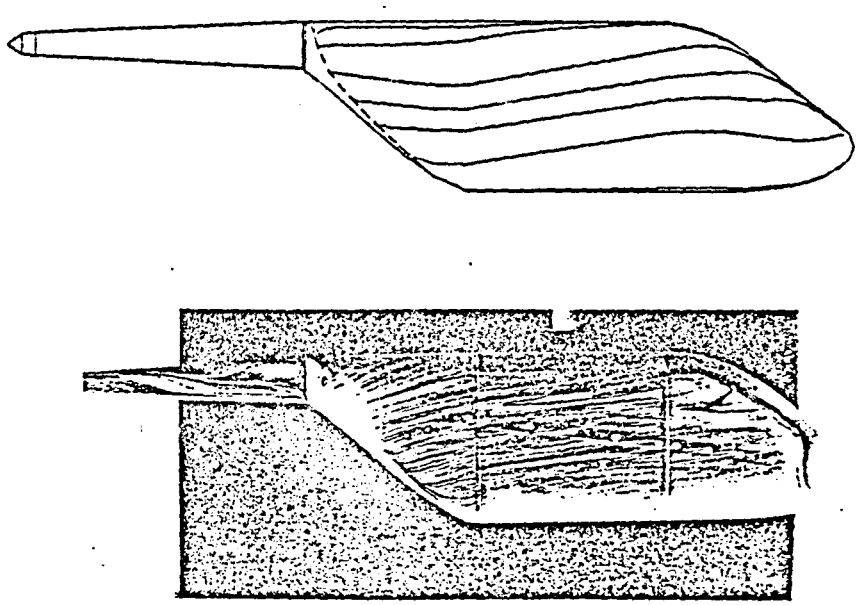

Fig. 20: Flow Profile at the Fuselage and Separation Line; Comparison of measurement and calculation

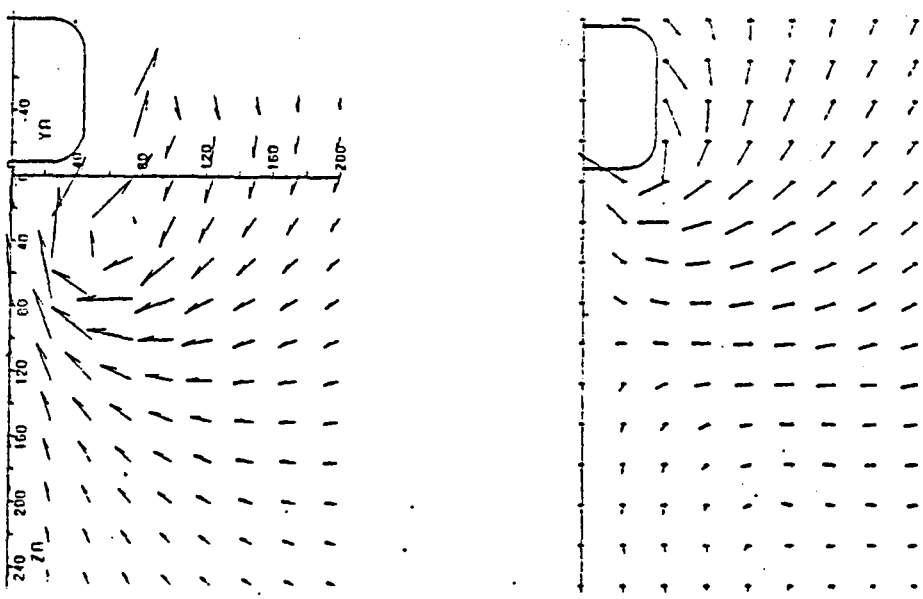

Figure 21: Velocity Field in Cross-plane behind the Fuselage of the Transport Helicopter Model

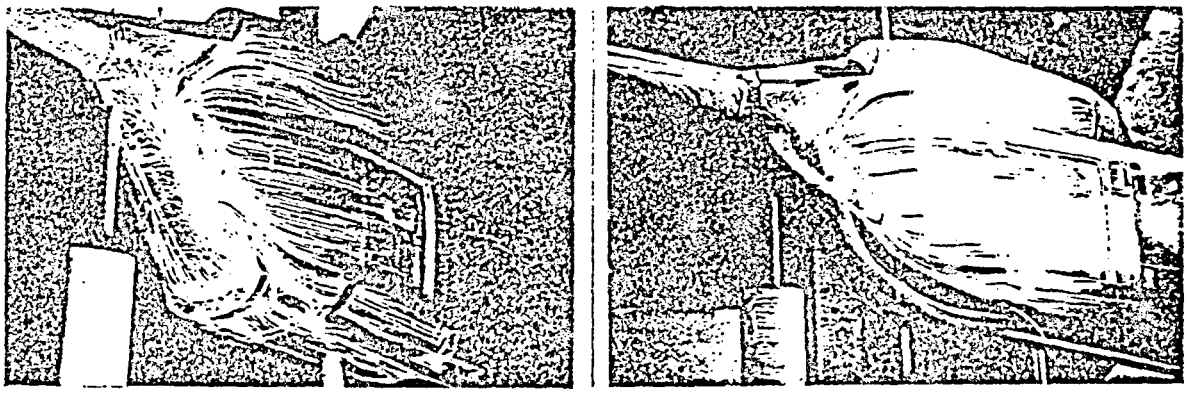

with spoiler $\alpha = -4°$ without spoiler

Figure 22: BK 117. Model with and without Spoiler

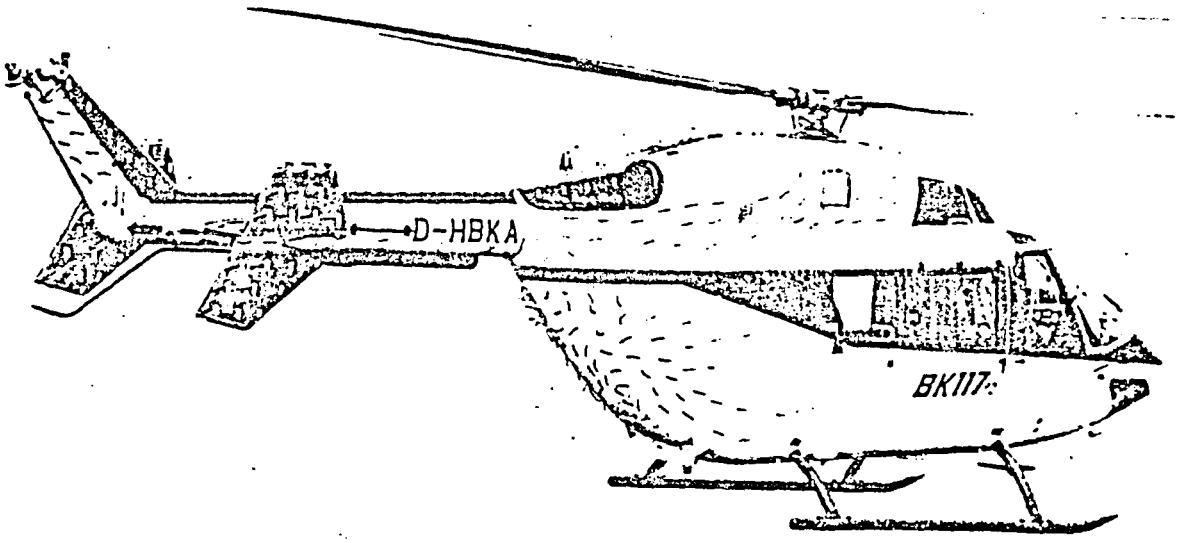

Descent at 80 kn

Figure 23: BK 117. Flow made Visible by Woll Threads

End of Document